ORIGINAL RESEARCH

Colchicine Ameliorates Dilated Cardiomyopathy Via SIRT2-Mediated Suppression of NLRP3 Inflammasome Activation

Xuan Sun (iD), PhD; Junfeng Duan, MD; Chenyi Gong, MD; Yuting Feng, MD; Jiaxin Hu, MD; Rong Gu, MD, PhD; Biao Xu (iD), MD, PhD

BACKGROUND: Dilated cardiomyopathy remains a leading cause of heart failure worldwide. Immune inflammation response is recognized as a significant player in the progression of heart failure; however, immunomodulatory strategies remain a long-term challenge. Colchicine, a potent anti-inflammatory drug, has many benefits in ischemic cardiovascular events, but its role in nonischemic heart failure remains unclear.

METHODS AND RESULTS: Doxorubicin administration was used to establish a murine dilated cardiomyopathy model, and colchicine or saline was orally given. At the end point, cardiac function and fibrosis were measured to investigate the effects of colchicine. Inflammatory cytokine levels, neutrophil recruitment, and NLRP3 (NOD-like receptor protein 3) inflammasome activation were detected to evaluate the inflammatory response. Furthermore, to examine the downstream target of colchicine, SIRT2 (Sirtuin 2) was pharmacologically inhibited in vitro; thus, changes in the NLRP3 inflammasome were detected by immunoblotting. These results showed that murine cardiac function was significantly improved and fibrosis was significantly alleviated after colchicine treatment. Moreover, the infiltration of neutrophils and the levels of inflammatory cytokines in the failing myocardium were both decreased by colchicine treatment. Mechanistically, colchicine upregulated the expression of SIRT2, leading to the inactivation of the NLRP3 inflammasome in an NLRP3 deacetylated manner. Conversely, the inhibition of SIRT2 attenuated the suppressive effect of colchicine on NLRP3 inflammasome activation.

CONCLUSIONS: This study indicated that colchicine could be a promising therapeutic candidate for dilated cardiomyopathy and other nonischemic heart failure associated with the inflammatory response.

Key Words: colchicine ■ dilated cardiomyopathy ■ inflammation ■ NLRP3 inflammasome ■ SIRT2

Dilated cardiomyopathy (DCM) is the leading cause of end-stage heart failure worldwide and is characterized by dilated ventricles and impaired heart contractility.[1,2] Clinically, the onset symptoms of patients with DCM are often insidious and get progressively worse. Although advances have been made in the treatment of patients with DCM in recent years, the prognosis is still poor. DCM is mainly caused by genetic abnormalities, toxic insults, viral infections, or other coronary heart disease risk factors.[3] The inflammatory response is central to the pathogenesis of DCM development and progression and ultimately results in adverse ventricular remodeling and impaired cardiac function.[4,5] Cumulating evidence indicates that DCM is recognized as a form of chronic or persistent cardiac inflammation triggered by proinflammatory stimuli, the most prominent being NLRP3 (NOD-like receptor protein 3) inflammasome activation.[6,7] Based on this,

CLINICAL PERSPECTIVE

What Is New?

- This study demonstrates that colchicine restrains the excess neutrophils accumulation and aberrant activation of the NLRP3 (NOD-like receptor protein 3) inflammasome during the progression of dilated cardiomyopathy in an SIRT2 (Sirtuin 2)-dependent manner.
- Inhibition of SIRT2 attenuates the colchicine-mediated anti-inflammatory effects and cardioprotective functions on dilated cardiomyopathy mice.

What Are the Clinical Implications?

- Our results provide the potential clinical application of colchicine in managing chronic dilated cardiomyopathy and other nonischemic heart failure associated with the inflammatory response.

Nonstandard Abbreviations and Acronyms

DCM	dilated cardiomyopathy
GDF15	growth and differentiation factor 15
NLRP3	NOD-like receptor protein 3
SIRT2	Sirtuin 2

exploration of anti-inflammatory strategies may be an effective measure against DCM.

Colchicine is a sophisticated, broad anti-inflammatory drug that has been applied for the prevention of gout for decades.[8] Recent clinical trials have demonstrated that low-dose colchicine has potential benefits in a range of coronary diseases because of its anti-inflammatory effect.[9] However, to date, it is still unclear whether colchicine could reduce the risk of progressive DCM. Colchicine is primarily taken up by leukocytes, especially neutrophils. The inhibition of inflammation with colchicine is mainly mediated through suppression of neutrophil chemoattraction, adhesion, migration, recruitment, and cytokine release in a combination of actions.[10] Furthermore, the molecular mechanism of colchicine has been reported to directly bind to tubulin heterodimers, interfere with microtubule stabilization, and alter the assembly of the NLRP3 inflammasome, leading to a reduction in the release of the proinflammatory cytokine interleukin-1β and other interleukins.[11] As a result, colchicine treatment could ameliorate systemic inflammation under pathological conditions. Nevertheless, the accurate underlying molecular mechanism involved in the colchicine effect has not yet been fully elucidated.

Modulation of chromatin by histone modifications has a strong impact on the regulation of inflammatory gene expression. Aberrant activation of the NLRP3 inflammasome is implicated in the acetylation switch under aging and overnutrition pathological conditions.[12] SIRTs (Sirtuins) are a family of class III nicotinamide adenine dinucleotide-dependent deacetylases that play a crucial role in regulating a diverse array of protein biochemistry and cellular functions.[13] SIRT2 (Sirtuin 2) resides in the nucleus and cytoplasm and is widely expressed throughout the body, especially in the heart.[13] According to the latest report, SIRT2 regulates 2 NLRP3 inflammasome downstream targets—NLRP3 and tubulin—and suggests that the deacetylation of NLRP3 and tubulin by SIRT2 leads to the inactivation of the NLRP3 inflammasome.[12,14] However, the impact of SIRT2 on the colchicine effect and the roles of SIRT2 in the progression of DCM remain unknown.

In the current study, we established this work to confirm that the anti-inflammatory drug colchicine could reduce the accumulation of neutrophils in DCM myocardium. Given that the deacetylase SIRT2 is involved in the regulation of the NLRP3 inflammasome, the present study aims to investigate whether SIRT2 is the downstream target of colchicine. Here, we showed that colchicine greatly protected cardiac function via SIRT2-mediated suppression of NLRP3 inflammasome activation during the progression of DCM. These results provide the potential clinical application of colchicine in managing chronic heart failure.

METHODS

The data that support the findings of this study are available from the corresponding author upon reasonable request and approval of the appropriate institutional review board.

Experimental Mice

C57BL/6 male mice were purchased (8 weeks of age) from Gem Pharmatech Co. Ltd (Jiangsu, China). Mice were maintained in the Animal Laboratory Resource Facility at Nanjing Drum Tower Hospital. All procedures on mice were approved by the Ethics Review Board for Animal Studies of Nanjing Drum Tower Hospital and performed in accordance with the guidelines set forth in the Guide for the Care and Use of Laboratory Animals published by the National Institutes of Health (Eighth Edition). After the study, all animals were anesthetized by isoflurane inhalation (1.5–2%) and then euthanized by cervical dislocation.

To establish chronic dilated cardiomyopathy model, mice were administered intraperitoneally with 5 mg/

kg doxorubicin (Sigma, St. Louis, MO, USA) weekly for consecutive 4 weeks at a cumulative dose of 20 mg/kg.[15] Colchicine (0.4 mg/kg, Selleck Chemicals LLC, Houston, TX, USA) or saline was given orally once daily for 4 weeks as described.[16] To inhibit the involvement of SIRT2 in vivo, a selective inhibitor of SIRT2, AGK2 (a reversible inhibitor of SIRT2) (1 mg/kg) was given intraperitoneally once daily for 4 weeks.[17] To assess mortality after doxorubicin challenge, mice surviving in each group were labeled as surviving mice/total mice.

Two-Dimensional Ultrasound Echocardiography

Cardiac function was assessed by transthoracic echocardiography with a VEVO 2100 Biomicroscope (VisualSonics). Mice were measured at 4 weeks following the first doxorubicin injection. Mice were anesthetized with isoflurane. End diastole was measured at the time of the apparent maximal left ventricular (LV) diastolic dimension, and end systole was measured at the time of the most anterior systolic excursion of the posterior wall. LV internal dimensions at end-diastole and at end-systole were measured digitally on the M-mode tracings and were averaged from 3 cardiac cycles. LV ejection fraction (%) and LV fractional shortening (%) were calculated. All measurements were made by one observer who was blinded with respect to the identity of the tracings.

Histological Analysis and Immunohistochemistry

After heart function assessment, mice were euthanized for histological study. Briefly, the LV myocardium (n=8 from each group) was fixed in 10% formalin, cut transversely, embedded in paraffin, sectioned into 5-μm slices and stained with hematoxylin and eosin for morphologic examination. Sirius red staining was also performed on heart tissue from different groups to observe the effects on myocardial fibrosis. Transverse sections were randomly obtained from the middle of the heart, and 5 randomly selected fields per section (n=8 each group) were analyzed. The collagen volume fraction was calculated as the sum of all areas containing connective tissue divided by the total area of the image by Image-Pro Plus 5.0.

The murine LV myocardium was excised and fixed with 10% formalin. The tissues were embedded in optimum cutting temperature compound (Tissue-Tek OCT) and serially cut into 5-μm slices. Cryosections were then blocked with PBS containing 5% bovine serum albumin and permeabilized with 0.1% Triton-X 100 in blocking solution. To detect the infiltration of neutrophils in the myocardium, heart sections were incubated with primary antibodies overnight at a dilution of 1:200 for Ly6G (lymphocyte antigen 6 complex locus G6D) (ab25377, Abcam) and 1:500 for cTNT (cardiac troponin T) (ab8295, Abcam) at 4 °C. To clarify the effect of colchicine on the

inflammasome, primary antibodies were added to heart sections overnight at a dilution of 1:100 for apoptosis-associated speck-like protein with CARD domain (PA5-95826, Invitrogen), 1:100 for NLRP3 (768319, Novus), and 1:100 for SIRT2 (19655-1-AP, Proteintech) at 4 °C. Secondary antibodies were added as follows: Alexa Flour 488 1:500 and Alexa Flour 647 1:500 for 2 hours at room temperature. Nuclei were counterstained with DAPI. Images were taken using a conventional fluorescence microscope (Leica Thunder, Germany). A total of 10 microscopic fields covering 1 mm^2 of the myocardial area were photographed, and the positive areas were counted by a blinded investigator.

RNA Extraction and Real-Time Polymerase Chain Reaction Analysis

Total mRNA was extracted using RNAiso plus (Vazyme Biotech Co. Ltd) according to the manufacturer's instructions. Real-time polymerase chain reaction (PCR) with SYBR Green, which was validated with respect to reproducibility and linearity within the measuring range, was performed in triplicate with the Cycler System (Applied Biosystems, USA), and Power SYBR Green PCR Master Mix (Vazyme Biotech Co. Ltd) was used as a reagent. To correct for potential variances between samples in mRNA extraction or in reverse transcribed efficiency, the mRNA content of each gene was normalized to the expression of the stably expressed reference gene GAPDH within the same sample. Sequences for all PCR primers are described in Table. Amplifications were performed using thermal

Table. Primer Sequences for Real-Time PCR Analysis

Gene name	Primer 5′-3′
GAPDH	Forward: AATGGATTTGGACGCATTGGT
	Reverse: TTTGCACTGGTACGTGTTGAT
Interleukin-1β	Forward: CCAGCTTCAAATCTCACAGCAG
	Reverse: CTTTGGGTATTGCTTGGGATC
Interleukin-6	Forward: ACAACGATGATGCACTTGCAGA
	Reverse: GATGAATTGGATGGTCTTGGTC
TNF-α	Forward: CAGGCGGTGCCTATGTCTC
	Reverse: CGATCACCCCGAAGTTCAGTAG
ANP	Forward: ACCTCCCGAAGCTACCTAAGT
	Reverse: CAACCTTTTCAACGGCTCCAA
BNP	Forward: CAGAAGCTGCTGGAGCTGATAAG
	Reverse: TGTAGGGCCTTGGTCCTTTG
NLRP3	Forward: ATTACCCGCCCGAGAAAGG
	Reverse: CATGAGTGTGGCTAGATCCAAG
SIRT2	Forward: GCGGGTATCCCTGACTTCC
	Reverse: CGTGTCTATGTTCTGCGTGTAG

ANP indicates atrial natriuretic peptide; BNP, brain natriuretic peptide; NLRP3, NOD-like receptor protein 3; PCR, polymerase chain reaction; SIRT2, Sirtuin 2; and TNF-α, tumor necrosis factor-alpha.

cycling conditions, including enzyme activation at 95 °C for 5 minutes, 40 cycles of denaturation at 95 °C for 10 seconds, and annealing/extension at 60 °C for 30 seconds. All samples were run in triplicate in 3 independent experiments. The relative expression level for each mRNA was calculated using the $2^{-\Delta\Delta Ct}$ method.

Flow Cytometry Analysis

For flow cytometry analysis, mice were euthanized (i.p. 120 mg/kg ketamine, 12 mg/kg xylazine, and 0.08 mg/kg atropine), blood samples were collected, and retrograde perfusion of hearts was performed using ice-cold PBS with 1% fetal bovine serum (FBS). Ventricles were dissected, rinsed in ice-cold PBS, and minced with Medimachine (BD Biosciences Pharmingen) in PBS with 1% FBS. Tissue suspensions were filtered through a 70-μm filter (BD Biosciences Pharmingen) and then centrifuged at 300g for 10 minutes at 4 °C. For staining, primary antibodies were added to the cells in a volume of 100 μL/10^6 cells and incubated for 45 minutes on ice in the dark. After incubation, the cells were washed and resuspended in 300 μL of PBS with 1% FBS. Then, the blood samples were treated with red blood cell lysis buffer. The data were collected on a FACS Caliber Flow cytometer (BD FACS Calibur, USA) and analyzed using Flow Jo 10.1 software (Tree Star). For fluorescence detection, blood neutrophils were incubated with an anti-mouse PE-labeled antibody against Ly6G (eBioscience) and a Percp-Cy5.5-labeled antibody against CD11b (eBioscience); heart neutrophils were incubated with an anti-mouse PE-labeled antibody against Ly6G (eBioscience) and an FITC-labeled antibody against CD45 (eBioscience).

ELISA Assays

Specimens of EDTA anticoagulated blood were collected and incubated at room temperature for 30 minutes on a rocking platform. Platelet-poor plasma was harvested by centrifugation at 2400g for 20 minutes at 4 °C and used to measure interleukin-1β (IL-1β), interleukin-6 (IL-6), and tumor necrosis factor-alpha (TNF-α) protein levels by commercial ELISA kits according to the manufacturer's instructions (Multi-Science, UK). Circulating GDF15 (growth and differentiation factor 15) protein levels was measured in the plasma by commercial ELISA kits according to the manufacturer's instructions (R&D, USA).

Cell Culture

Primary neutrophils were collected from bone marrow as described.[18] Briefly, bone marrow cells were collected from the femurs and tibias of 4-week-old mice by flushing with RPMI 1640 medium containing 10 U/mL heparin, 50 U/mL penicillin and 50 g/mL streptomycin. Then, the cells were treated with red blood cell lysis buffer and filtered through a 70-μm mesh. Resuspend the cell pellet in 200 μL of buffer per 5×10^7 total cells. Primary neutrophils were sorted from the cells by magnetic beads according to the manufacturer's instructions (130-097-658, Miltenyi Biotec). After washing with PBS, primary neutrophils were resuspended in RPMI 1640 (supplemented with 10% FBS, 50 U/mL penicillin, and 50 g/mL streptomycin) and then plated. The NB4 cell line (Chinese Academy of Sciences Cell Bank, Shanghai, China) was cultured in RPMI 1640 supplemented with 10% FBS, 50 U/mL penicillin, and 50 g/mL streptomycin.

To induce NLRP3 inflammasome activation in neutrophils, doxorubicin (5 μmol/L, Selleck Chemicals LLC),[6] and nigericin (10 μmol/L, MCE, NJ, USA)[19] were added to RPMI 1640 medium for 4 hours. In addition, neutrophils were incubated with or without colchicine (10 μmol/L, Selleck Chemicals LLC) for 4 hours.[20] To identify the role of SIRT2, the SIRT2 inhibitor AGK2 (10 μmol/L, MCE, NJ, USA) was added to RPMI 1640 medium for 4 hours.[21]

Cell Viability Assay

The viability of the isolated neutrophils after drug stimulation was detected by Cell Counting Kit 8 assay kit according to the manufacturer's instructions (CK04, Dojindo, Kumamoto, Japan). Neutrophils were counted and ≈2000 cells per well were seeded in a 96-well plates with RPMI 1640 medium containing 10 U/mL heparin, 50 U/mL penicillin and 50 g/mL streptomycin. Then neutrophils were treated with drugs under the same conditions as described above. Afterwards, 10 μL of the Cell Counting Kit 8 reagent was added to each well and incubated for 2 hours at 37 °C. Absorbance measurements were taken at dual wavelength with detection wavelength at 450 nm and reference wavelength at 650 nm using a Tecan Infinite M200 microplate reader (LabX, Austria). The measurements at 450 nm minus that at 650 nm were used for calculating. The percentage each concentration accounted for of the control was presented as cell viability.

Western Blot

To check the effect of colchicine on the NLRP3 inflammasome via SIRT2 activation, we detected the expression of SIRT2 and the NLRP3 inflammasome pathway in heart tissues and primary neutrophils. Heart tissues were lysed in RIPA buffer (Sigma Aldrich), and total protein was quantified by bicinchoninic acid assay (Thermo Fisher Scientific). Samples were separated by 8% to 12% SDS–PAGE with Mini Protean

precast gels (Bio–Rad Laboratories). Protein homogenates were subjected to analysis using antibodies against SIRT2 (19655-1-AP, Proteintech), acetylated lysine (623402, Biolegend), NLRP3, absent in melanoma 2, apoptosis-associated speck-like protein with card domain, pro-IL-1β, cleaved IL-IL1β, caspase-1, cleaved caspase-1 (20836, CST) and GAPDH (5174, CST). Then, the cells were incubated with horseradish peroxidase-labeled anti-rabbit immunoglobulin G or horseradish peroxidase-labeled anti-mouse immunoglobulin G. The signals were detected with an electrochemiluminescence ECL system (Amersham) and quantified by scanning densitometry with an ImageJ analysis system.

Immunoprecipitation

Cardiac tissue protein lysates were obtained using immunoprecipitation (IP) lysis buffer containing protease inhibitor (Absin Bioscience, Shanghai, China). Lysates were then incubated with Protein A/G agarose beads (Absin Bioscience, Shanghai, China). Samples
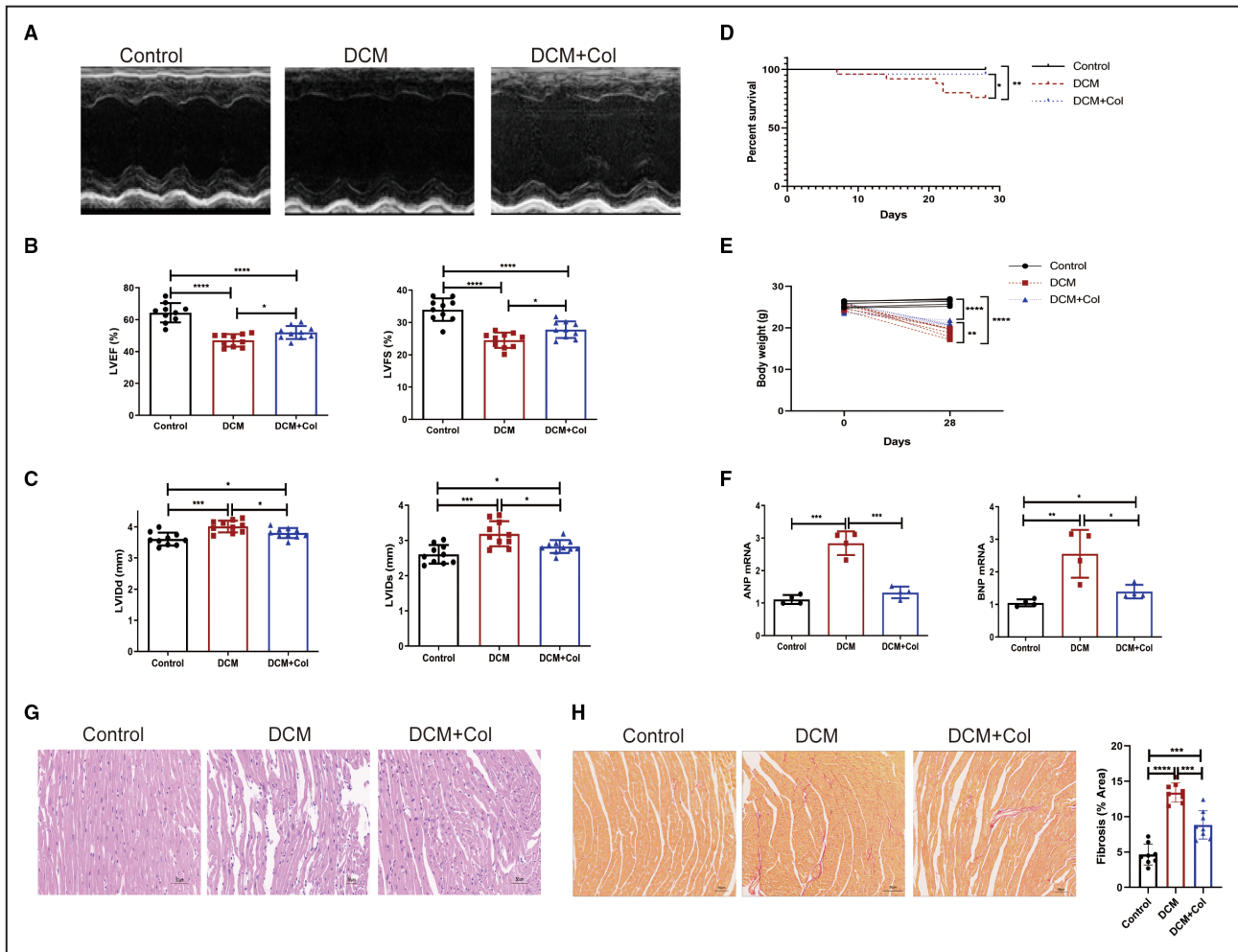

Figure 1. Colchicine treatment significantly improved murine cardiac functions.
A through **C**, Cardiac function is analyzed by 2-dimensional murine echocardiography, left ventricular (LV) ejection fraction, LV fractional shortening, LV internal dimensions at end-diastole, and LV internal dimensions at end-systole values are measured at the end point of experiment (n=10 each group). **D**, Kaplan-Meier survival curve for each group mice followed for 4 weeks with or without doxorubicin challenge (n=25 each group). **E**, The changes of body weight from beginning to end (n=6 each group). **F**, Relative expression of *ANP* (atrial natriuretic peptide) mRNA and *BNP* (brain natriuretic peptide) mRNA are normalized to *GAPDH* mRNA in murine cardiac tissues at the end point of experiment. **G** and **H**, The representative hematoxylin and eosin staining (**G**) and Sirius red staining (**H**) of hearts in each group are shown. Quantification of interstitial fibrosis (% area) in hearts is shown on the right; n=8 each group. Five images per mouse are evaluated. Scale bar=50 µm. Data are shown as mean±SEM. Data of (**B**, **C**, and **E** through **G**) are analyzed by 1-way ANOVA (Tukey post-test). Data of (**D**) is analyzed by Mantel-Cox test. ANP indicates atrial natriuretic peptide; BNP, brain natriuretic peptide; DCM, dilated cardiomyopathy; LVEF, left ventricular ejection fraction; LVFS, left ventricular fractional shortening; LVIDd, left ventricular internal dimensions at end-diastole; and LVIDs, left ventricular internal dimensions at end-systole. *P<0.05 between groups; **P<0.01 between groups; ***P<0.005 between groups; and ****P<0.001 between groups. Col indicates colchicine.

were immunoprecipitated using anti-NLRP3 antibody (15101,CST) or normal rabbit immunoglobulin G (2729S, CST) overnight at 4 °C. Immunoprecipitates were washed with lysis buffer 3 times. Laemmli sample buffer (Bio–Rad) was then added, and samples were boiled, separated by SDS–PAGE, and immunoblotted.

The granulocyte cell line NB4 was transfected with the NLRP3-Flag plasmid. Then, cell lysates were obtained via IP lysis buffer containing protease inhibitor (Absin Bioscience, Shanghai, China). Cell lysates were then incubated with Protein A/G agarose beads (Absin Bioscience, Shanghai, China). Then, samples were immunoprecipitated with anti-Flag antibody (F1804, Sigma) or normal rabbit immunoglobulin G (2729S, CST) overnight at 4 °C. Immunoprecipitates were washed with lysis buffer 3 times and eluted with Flag peptide. Laemmli sample buffer (Bio–Rad) was then added, and samples were boiled, separated by SDS–PAGE, and immunoblotted.

Statistical Analysis

Data from at least 3 independent experiments are presented as the mean±SD, unless otherwise indicated. To determine differences between groups, data were tested using either 1-way ANOVA followed by Tukey multiple comparisons test or 2-way ANOVA followed by Bonferroni multiple comparisons test. To determine differences between groups in Kaplan–Meier survival curves, data were tested using the Mantel-Cox test. All analyses were performed using Prism 6 software (GraphPad), and only differences with a *P* value of <0.05 were considered statistically significant.

RESULTS

Colchicine Treatment Alleviates Cardiac Damage in Doxorubicin-Induced Mice

To verify the effect of colchicine on chronic heart failure, cardiac function parameters were measured by echocardiography. Compared with the control group, the DCM group mice exhibited a pronounced decrease in LV ejection fraction (47.08±3.89% versus 64.35±6.07%; *P*<0.001) and LV fractional shortening

(24.52±2.37% versus 33.99±3.48%; *P*<0.001), further leading to impaired contractile function with dilated left ventricle, but colchicine treatment significantly rescued the depressed LV ejection fraction (51.94±4.04% versus 47.08±3.89%; *P*<0.05) and LV fractional shortening (27.77±2.56% versus 24.52±2.37%; *P*<0.05), as well as ventricular expansion, compared with the DCM group (Figure 1A through 1C). During the entire experiment, mice were followed up after doxorubicin challenge to assess mortality. There were 80% of DCM mice survived for 4 weeks, while 96% of colchicine treated DCM mice survived (Figure 1D). In addition, colchicine treatment prevented the weight loss induced by doxorubicin insults (Figure 1E). Quantitative real-time PCR analysis showed that there were lower mRNA levels of *ANP* (atrial natriuretic peptide: 1.33±0.18 versus 2.84±0.36; *P*=0.0003) and *BNP* (brain natriuretic peptide: 1.39±0.20 versus 2.56±0.73; *P*=0.0229) in the colchicine treatment group than in the DCM group (Figure 1F). Hematoxylin and eosin staining showed more necrotic cardiomyocytes and disturbed cardiac fibers in the DCM group than in the colchicine treatment group; Sirius red staining showed that cardiac fibrosis was significantly increased in the DCM group compared with the colchicine treatment group (13.41±1.36 versus 8.85±2.00; *P*<0.0001) (Figure 1G and 1H). Besides, the usage of colchicine in our studies were proven to be safe as shown that mice in the sole colchicine treatment group did not show any difference compared with the control mice in cardiac function and survival rate (Figure S1). Taken together, colchicine treatment alleviated cardiac structural remodeling and mechanical dysfunction during DCM progression. Meanwhile, we observed a modest survival benefit in colchicine treatment.

Colchicine Treatment Limits Neutrophil Infiltration in the Failing Myocardium

We investigated the levels of inflammatory cytokines in the circulating and myocardium. Compared with the DCM group, the circulating levels of IL-1β, IL-6, and TNF-α were significantly downregulated after colchicine treatment (Figure 2A). GDF15 is a novel promising anti-inflammatory biomarker associated with outcome in patients with heart failure.[22,23] Our results showed that

Figure 2. Colchicine reduced the recruitment of neutrophils.

A, ELISA analysis of inflammatory factor interleukin-1, interleukin-6, and tumor necrosis factor-α in murine plasma at the end point of experiment (n=8–12 each group). **B**, ELISA analysis of GDF15 in murine plasma at the end point of experiment (n=8–12 each group). **C**, Relative expression of inflammatory cytokine *interleukin-1* mRNA, *interleukin-6* mRNA, and *tumor necrosis factor-α* mRNA are normalized to *GAPDH* mRNA in murine cardiac tissues at the end point of experiment (n=5 each group). **D** and **E**, Representative flow cytometric and statistical analysis of CD11b⁺Ly6G⁺ neutrophil in the blood (**D**) and CD45⁺Ly6G⁺ neutrophil in the heart € (n=6 each group). **F**, Representative immunofluorescence images of cardiac tissues staining with Ly6G (green), cTNT (cardiac troponin T) (red), and DAPI (blue). Frequency of Ly6G-positive neutrophils is shown on the right (n=6–8 each group). Five images per mouse are evaluated. Scale bar=50 µm. Data are shown as mean±SEM. All data statistical significance are determined by 1-way ANOVA (Tukey post-test). cTNT indicates cardiac troponin T; DCM, dilated cardiomyopathy; GDF15, growth and differentiation factor 15; IL-1, interleukin-1; IL-6, interleukin-6; and TNF-α, tumor necrosis factor-α. *P<0.05 between groups; **P<0.01 between groups; ***P<0.005 between groups; and ****P<0.001 between groups. Col indicates colchicine; Ly6G, lymphocyte antigen 6 complex locus G6D.
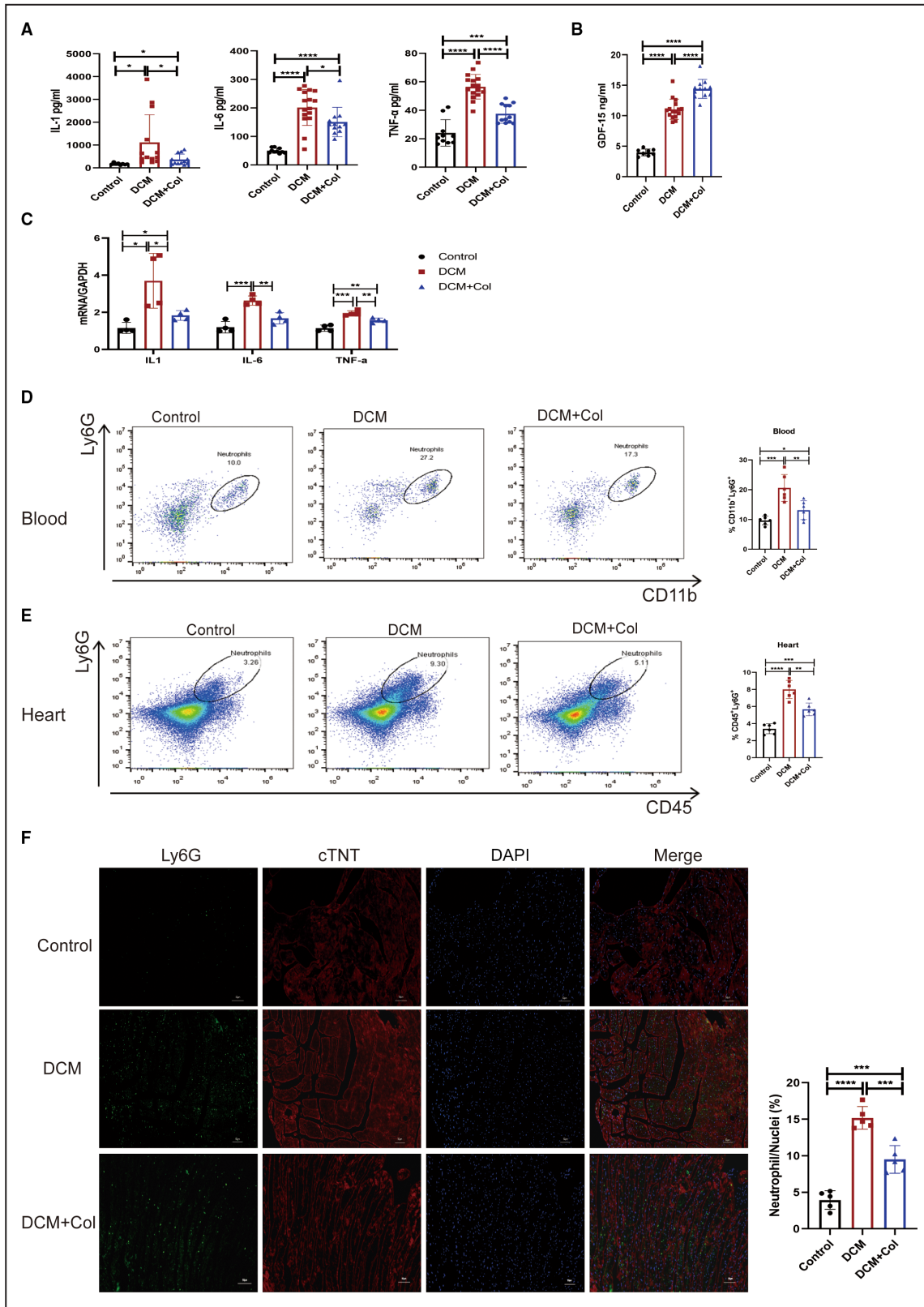
colchicine treatment increased the secretion of circulating GDF15 (14.41±1.55% versus 11.06±1.65%; *P*<0.001) in DCM mice (Figure 2B). In consistent with the circulating results, quantitative real-time PCR analysis showed that there were lower mRNA levels of *IL-1β* (1.83±0.26 versus 3.69±1.48; *P*=0.0474), *IL-6* (1.66±0.30 versus 2.65±0.26; *P*=0.0025), and *TNF-α* (1.566±0.12 versus 1.94±0.13; *P*=0.0062) in the colchicine treatment heart

than in the DCM heart (Figure 2C). Next, we focused on the changes of neutrophils, which identified as the target cell of colchicine. Representative flow cytometry gates for identification of circulating and cardiac CD45+ cells and neutrophils were depicted in Figure S2A, S2B and Figure 2D and 2E. Flow cytometry analysis revealed that colchicine significantly inhibited doxorubicin-induced neutrophil accumulation in the blood (CD11b+Ly6G+) and myocardium (CD45+Ly6G+) (Figure 2D and 2E). Immunofluorescent staining of heart tissues confirmed that neutrophil infiltration in the myocardium was distinctly reduced by colchicine treatment (Figure 2F).

NLRP3 Inflammasome Activation Is Repressed by Colchicine Treatment

Given that the NLRP3 inflammasome plays a vital role in the pathophysiology of DCM, we detected the protein levels of the NLRP3 inflammasome pathway in the murine myocardium. We found that doxorubicin enhanced the expression of the NLRP3 inflammasome pathway in cardiac tissue, but colchicine led to a decline in NLRP3 inflammasome activation by doxorubicin (Figure 3A and 3B). Besides, the plasma level and cardiac expression of IL-1β induced by doxorubicin injection was significantly blunted by colchicine treatment (Figure 2A and 2C). Consistent with the western blotting analysis, immunofluorescent staining indicated that apoptosis-associated speck-like protein with card domain specks in DCM myocardium were also attenuated by colchicine treatment (10.90±1.66% versus 6.33±1.10%; *P*=0.0009) (Figure 3C).

Expression of SIRT2 Is Increased by Colchicine Treatment

It has been reported that histone deacetylase SIRT2 inactivation leads to NLRP3 acetylation, which contributes to NLRP3 inflammasome activation in aging mice.[12] We sought to clarify whether the anti-inflammatory effect of colchicine was related to SIRT2 activation. Immunoprecipitation was performed to pull down the acetylated proteins in the murine cardiac tissues via acetylated lysine-specific antibody. Compared with the control hearts, the acetylation level of NLRP3 was increased in the DCM group. In addition, doxorubicin induced an obvious downregulation of SIRT2 in cardiac tissues. However, colchicine treatment inhibited NLRP3 acetylation and potentiated the induction of SIRT2, suggesting that colchicine protects against SIRT2 inactivation induced by doxorubicin (Figure 4A). Quantitative real-time PCR analysis also showed that there was higher mRNA level of *SIRT2* in the colchicine treatment heart than in the DCM heart (0.83±0.07 versus 0.49±0.05; *P*=0.0004) (Figure 4B).

We future verified the effect of SIRT2 in vitro. Primary neutrophils were isolated from bone marrow via magnetic bead separator. The isolation purity of sorted neutrophils was shown in Figure S2C. Then primary neutrophils were stimulated with or without doxorubicin and the NLRP3 inflammasome activator nigericin and incubated with or without colchicine minus or plus the SIRT2 inhibitor AGK2 for 4 hours. Impacts of these drug treatments on the viability of isolated neutrophils were detected by the Cell Counting Kit 8 assay kit (Figure S2D). Compared with the control group, the mRNA levels of *IL-1β* and *NLRP3* were increased in the group stimulated with doxorubicin and nigericin and then decreased in the colchicine treatment group, and AGK2 blunted the effect of colchicine (Figure 4C). In parallel with the mRNA results, western blotting analysis showed that colchicine decreased NLRP3 inflammasome activation induced by doxorubicin and nigericin, while AGK2 reversed this reduction effect of colchicine, suggesting that SIRT2 was involved in colchicine regulation (Figure 4D).

Colchicine Promotes the Deacetylation of NLRP3 by Enhancing the Expression of SIRT2

We wondered whether colchicine contributed to the deacetylation of NLRP3 by SIRT2. Dual immunostaining of SIRT2 and NLRP3 was performed in myocardial sections. The expression of NLRP3 was obviously increased and the expression of SIRT2 was significantly decreased in DCM heart tissues. In contrast, colchicine attenuated the activation of NLRP3, and the combination of SIRT2 with NLRP3 was remarkably elevated (Figure 5A). Consistent with in vivo studies, we found that colchicine treatment significantly decreased NLRP3 activation and increased SIRT2 expression (Figure 5B). Interestingly, the alteration of SIRT2 and NLRP3 induced by colchicine was inhibited by AGK2 upon doxorubicin and nigericin stimulation (Figure 5B). To determine whether colchicine was involved in the deacetylated effect of SIRT2 on NLRP3, we assessed the deacetylation of NLRP3 by IP. The granulocyte cell line NB4 was transfected with NLRP3-Flag plasmids, NB4 cells were treated with or without colchicine and AGK2 upon doxorubicin and nigericin stimulation, and cell lysates were immunoprecipitated using an anti-Flag antibody. After that, we used an anti-acetylated lysine antibody for examination by immunoblots. The protein results suggested that the deacetylation of NLRP3 was enhanced in cells stimulated with doxorubicin and nigericin (Figure 5C). However, acetylation was decreased by colchicine treatment, while suppression of SIRT2 by AGK2 reversed the colchicine effect (Figure 5C).
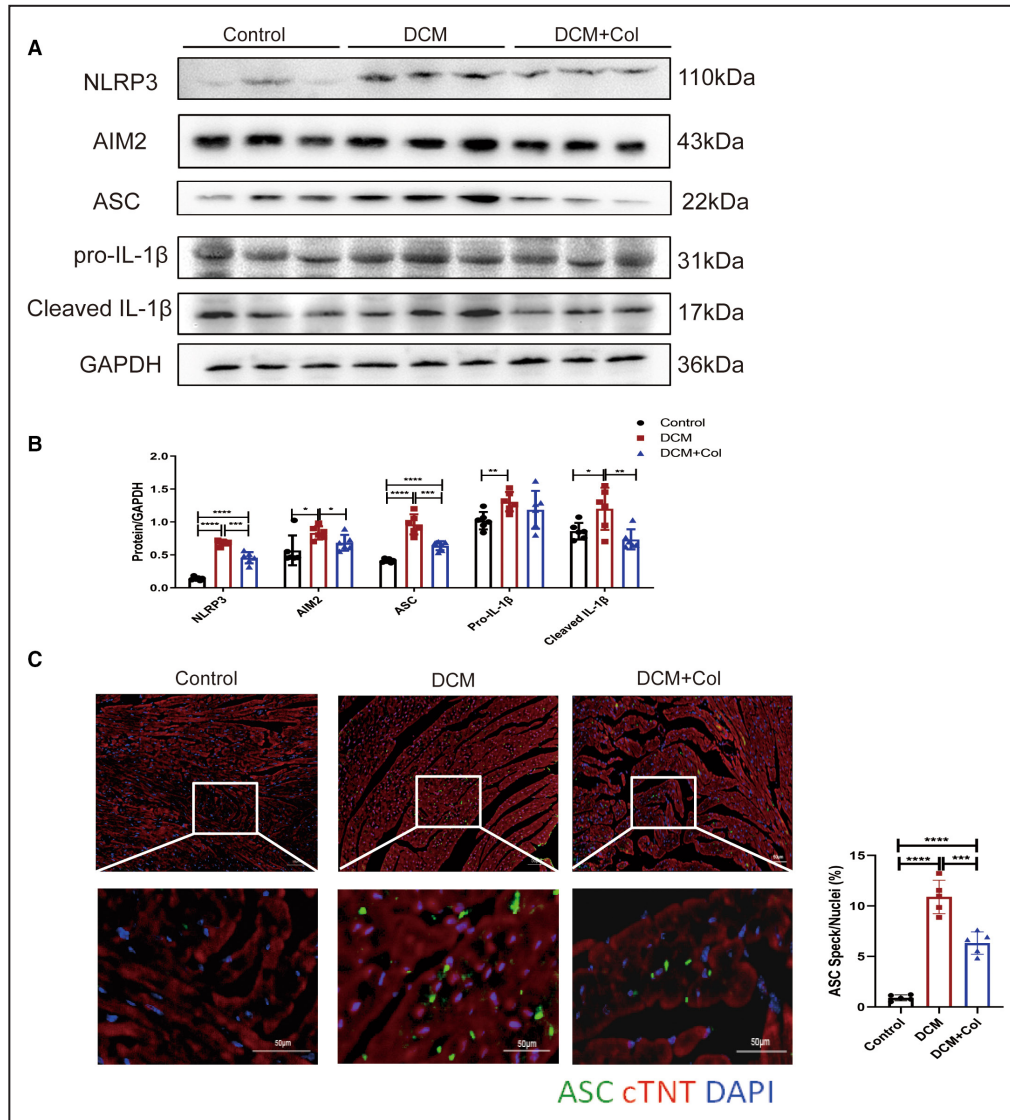
Figure 3. NLRP3 (NOD-like receptor protein 3) inflammasome pathway was inhibited by colchicine treatment.
A and **B**, Representative immunoblots and the corresponding analysis of NLRP3 inflammasome pathway in cardiac tissues at the end point of experiment. GAPDH shows as loading control. **C**, Representative immunofluorescence images of cardiac tissues staining with ASC (green), cTNT (cardiac troponin T) (red), and DAPI (blue). Frequency of ASC speck is shown on the right (n=6–8 each group). Five images per mouse are evaluated. Scale bar=50 μm. Data are shown as mean±SEM. All data statistical significance are determined by 1-way ANOVA (Tukey post-test). cTNT indicates cardiac troponin T; DCM, dilated cardiomyopathy; IL-1β, interleukin-1β; and NLRP3, NOD-like receptor protein 3. *$P<0.05$ between groups; **$P<0.01$ between groups; ***$P<0.005$ between groups; and ****$P<0.001$ between groups. AIM2 indicates absent in melanoma 2; ASC, apoptosis-associated speck-like protein with CARD domain; Col, colchicine.

Inhibition of SIRT2 In Vivo Attenuates the Advantageous Effects of Colchicine During the Progression of DCM

To investigate the involvement of SIRT2 in the colchicine-dependent action in vivo, doxorubicin-treated mice were given with colchicine and AGK2 simultaneously. The western blotting results showed that AGK2 treatment obviously reduced the expression of SIRT2 in the heart, suggesting a successful inhibition of SIRT2 in vivo (Figure S3). Echocardiography measurements results showed that the inhibition of SIRT2 by AGK2 reversed the cardiac improvement of colchicine in DCM mice (Figure 6A through 6C). In addition, AGK2 treatment abolished the benefits of survival rate and weight loss brought by colchicine (Figure 6D and 6E). The cardiac expression of *ANP* (2.71±0.58 versus 1.67±0.36; $P=0.0024$) and *BNP* (3.95±1.19
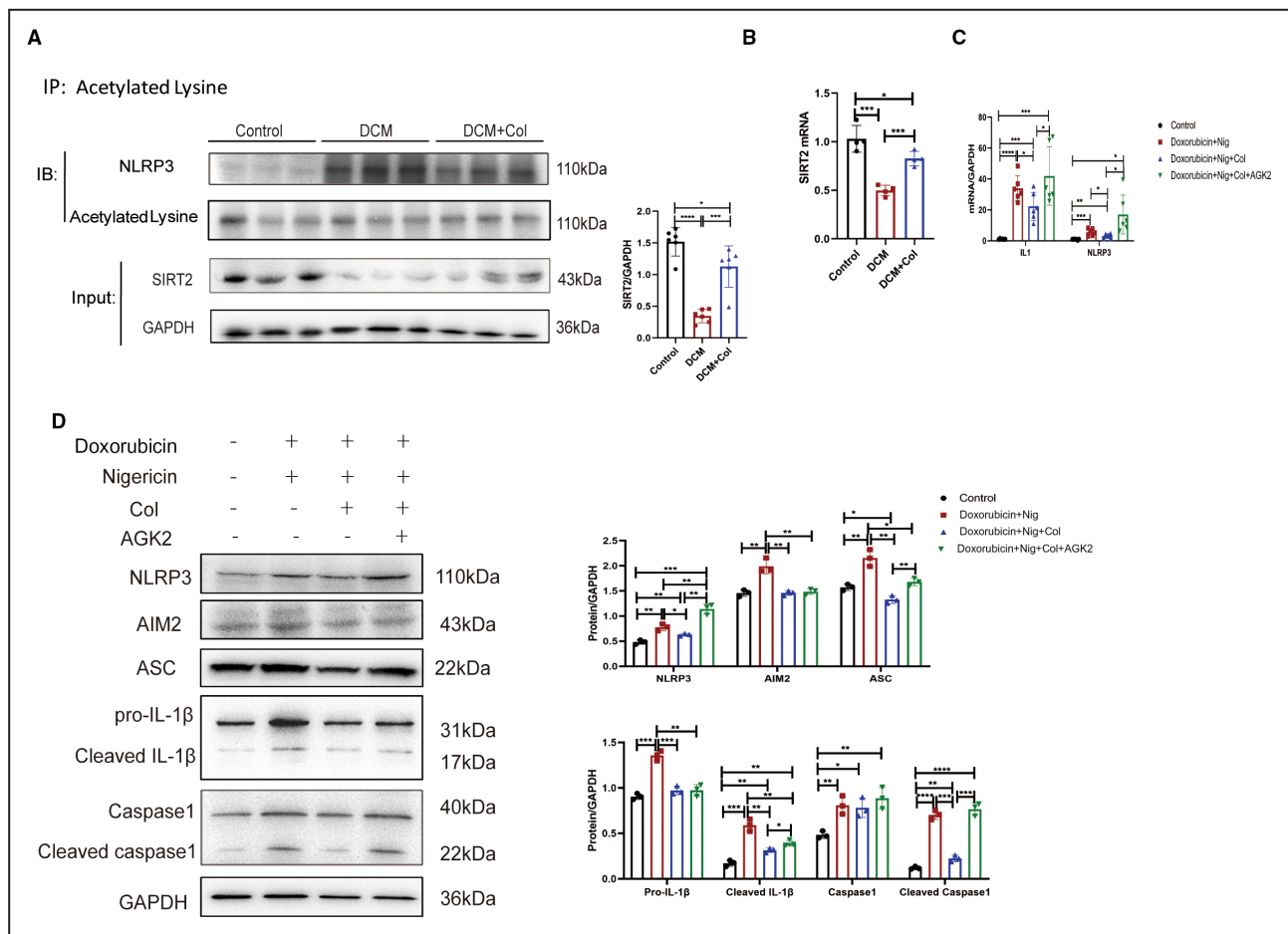
Figure 4. SIRT2 (Sirtuin 2) is involved in the anti-inflammation effect of colchicine.
A, Acetylated NLRP3 (NOD-like receptor protein 3) levels in the cardiac tissues of mice at the end point of experiment. Immunoglobulin G is the negative control and GAPDH is the input loading control. Data are representative of 3 independent experiments. Western blot analysis on expression of SIRT2 in cardiac tissues at the end of experiment (n=6 each group) on the right. **B**, Relative expression of *SIRT2* mRNA is normalized to *GAPDH* mRNA in cardiac tissues (n=4 each group). **C**, Relative expression of inflammatory cytokine *interleukin-1* mRNA and *NLRP3* mRNA are normalized to *GAPDH* mRNA in primary neutrophil that are treated +/− colchicine (10 µmol/L, 2 hours), +/− SIRT2 inhibitor AGK2 (10 µmol/L, 2 hours) or challenged with doxorubicin (5 µmol/L, 2 hours) and inflammasome activators nigericin (10 µmol/L, 2 hours); n=6 each group. **D**, Western blot analysis on expression of NLRP3 inflammasome pathway in primary neutrophil that are treated +/− colchicine (10 µmol/L, 2 hours), +/− SIRT2 inhibitor AGK2 (10 µmol/L, 2 hours) or challenged with doxorubicin (5 µmol/L, 2 hours) and inflammasome activators nigericin (10 µmol/L, 2 hours). GAPDH shows loading control. Data are representative of 3 independent experiments. Data are shown as mean±SEM. Data of (**A** and **B**) are analyzed by 1-way ANOVA (Tukey post-test). Data of (**C** and **D**) are analyzed by 2-way ANOVA (Bonferroni post-test). DCM indicates dilated cardiomyopathy; IL-1β, interleukin-1β; NLRP3, NOD-like receptor protein 3; and SIRT2, Sirtuin 2. *P<0.05 between groups; **P<0.01 between groups; ***P<0.005 between groups; and ****P<0.001 between groups. AGK2 indicates a reversible inhibitor of SIRT2; AIM2, absent in melanoma 2; ASC, apoptosis-associated speck-like protein with CARD domain; Col, colchicine; IB, immunoblot; IP, immunoprecipitation; Ly6G, lymphocyte antigen 6 complex locus G6D.

versus 1.88±0.39; *P*=0.0039) were both increased in the AGK2-added group (Figure 6F). Hematoxylin and eosin staining showed that cardiomyocytes in the DCM mice injected with both colchicine and AGK2 were displayed as disturbed sarcomeres and necrotic debris (Figure 6G). At the same time, Sirus red staining showed that the degree of cardiac fibrosis was more severe in the AGK2-added group (15.50±3.21 versus 11.03±2.40; *P*=0.0072) (Figure 6H). These above results demonstrated that inhibition of SIRT2 via AGK2

abrogated the cardioprotective effects of colchicine during the progression of DCM in vivo.

DISCUSSION

Collectively, we demonstrated that colchicine treatment prevented the deterioration of cardiac function and myocardial damage due to its anti-inflammatory properties in a murine DCM model. Colchicine treatment
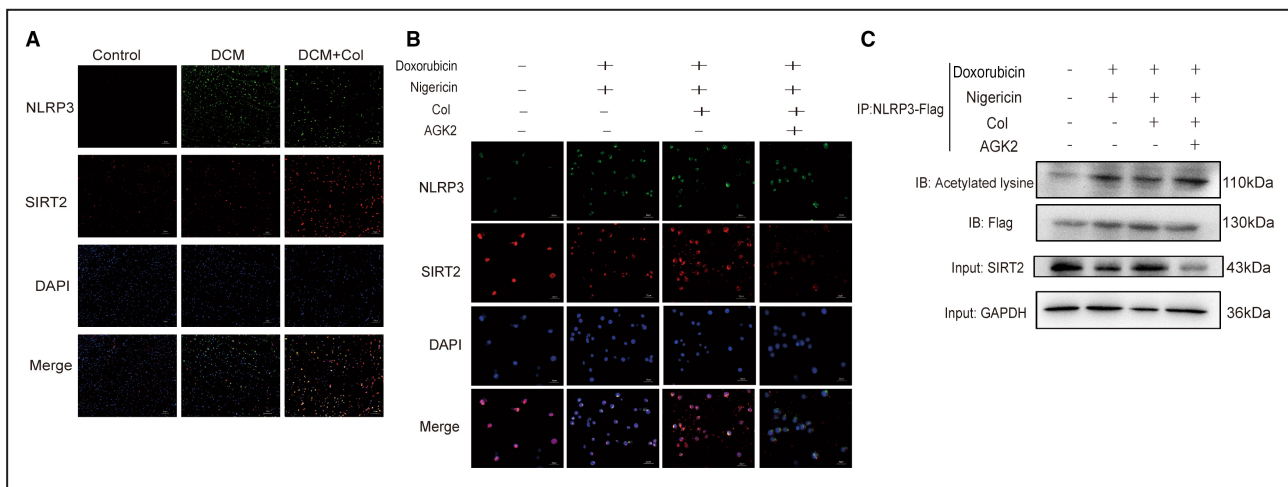
Figure 5. **Colchicine promotes the deacetylation of NLRP3 (NOD-like receptor protein 3) by SIRT2 (Sirtuin 2).**
**A**, Representative immunofluorescence images of cardiac tissues staining with NLRP3 (green), SIRT2 (red), and DAPI (blue). (n=6–8 each group). Five images per mouse are evaluated. Scale bar=50 μm. **B**, Representative immunofluorescence images of primary neutrophils that are treated +/− colchicine (10 μmol/L, 2 hours), +/− SIRT2 inhibitor AGK2 (10 μmol/L, 2 hours) or challenged with doxorubicin (5 μmol/L, 2 hours) and inflammasome activators nigericin (10 μmol/L, 2 hours). NLRP3 (green), SIRT2 (red) and DAPI (blue). Scale bar=20 μm. Data are representative of 3 independent experiments. **C**, The effect of SIRT2 on the deacetylation of NLRP3 is evaluated by coimmunoprecipitation. NLRP3-Flag plasmid is transfected into NB4 cell line, then NB4 cell line is treated with +/− colchicine (10 μmol/L, 2 hours), +/− SIRT2 inhibitor AGK2 (10 μmol/L, 2 hours) or challenged with doxorubicin (5 μmol/L, 2 hours) and inflammasome activators nigericin (10 μmol/L, 2 hours). Cell lysates are immunopurified with anti-Flag antibody. Then the expression of acetylated lysine is measured by IP. GAPDH is the input loading control. Data are representative of 3 independent experiments. DCM indicates dilated cardiomyopathy; IL-1β, interleukin-1β; NLRP3, NOD-like receptor protein 3; and SIRT2, Sirtuin 2. AGK2, a reversible inhibitor of SIRT2; Col, colchicine; IB, immunoblot; IP, Immunoprecipitation.

remarkably prohibited the infiltration of neutrophils into the injured myocardium and attenuated the inflammatory response. Furthermore, we found that colchicine protected SIRT2 from doxorubicin-induced inactivation and contributed to the deacetylation of NLRP3, which resulted in the suppression of the NLRP3 inflammasome. Importantly, a SIRT2 inhibitor blunted colchicine-mediated cardioprotective functions, indicating that SIRT2 was a vital downstream mediator of colchicine.

In general, DCM manifests as a chronic, low-grade cardiac inflammation disease. During dilated cardiomyopathy, accumulated activated immune cells and sustained release of proinflammatory cytokines contribute to myocardial inflammation and ventricular remodeling.[24,25] As a result, there is an urgent need to identify immunomodulatory strategies to treat patients with heart failure. Recently, a series of clinical trials of the anti-inflammatory drug colchicine in patients with acute and chronic coronary disease demonstrated that the use of colchicine at doses of 0.5–1.0 mg daily has beneficial cardiovascular efficacy, indicating that colchicine can be used for secondary prevention in cardiovascular disease.[9,26] Nonetheless, trials exploring the effect of colchicine on heart failure are limited to a single randomized controlled trial, and 2 other clinical trials are ongoing.[27] Our studies provided distinct preclinical evidence that colchicine reduced the risk of ventricular remodeling and slowed the progression of DCM.

In the rat sterile pericarditis model, it was reported that the benefits of colchicine were seen soon after the therapy outset and continued over the course[28]; however, the protective effect of colchicine was lost if treatment was started late,[29] suggesting the initial suppression of inflammation by colchicine. Neutrophils are the first cells to arrive at cardiac inflammation sites, and since they are short-lived, sustained neutrophil recruitment is ongoing in processive heart failure.[30,31] In this study, when colchicine was given at the beginning of doxorubicin insults, neutrophil numbers in the blood and heart were both significantly reduced, which demonstrated the potent anti-inflammatory ability of colchicine in the initiation phases of cardiac inflammation.

Our results showed that colchicine treatment reduced both circulatory and cardiac levels of proinflammatory IL-1, IL-6, as well as TNF-α and increased the secretion of circulating GDF15 in DCM mice, suggesting a strong systemic anti-inflammation effect of colchicine. Emerging evidences have demonstrated that GDF15 is served as a novel cardiac anti-inflammatory biomarker in cardiovascular disease.[22] GDF15 is not expressed in the normal adult heart but is induced in response to specific conditions like dilated cardiomyopathy.[32,33] It has been reported that GDF15 is required for the anti-inflammatory action of colchicine,[34] indicating that colchicine could affect both cardiac and systemic inflammation (Figure 2B).
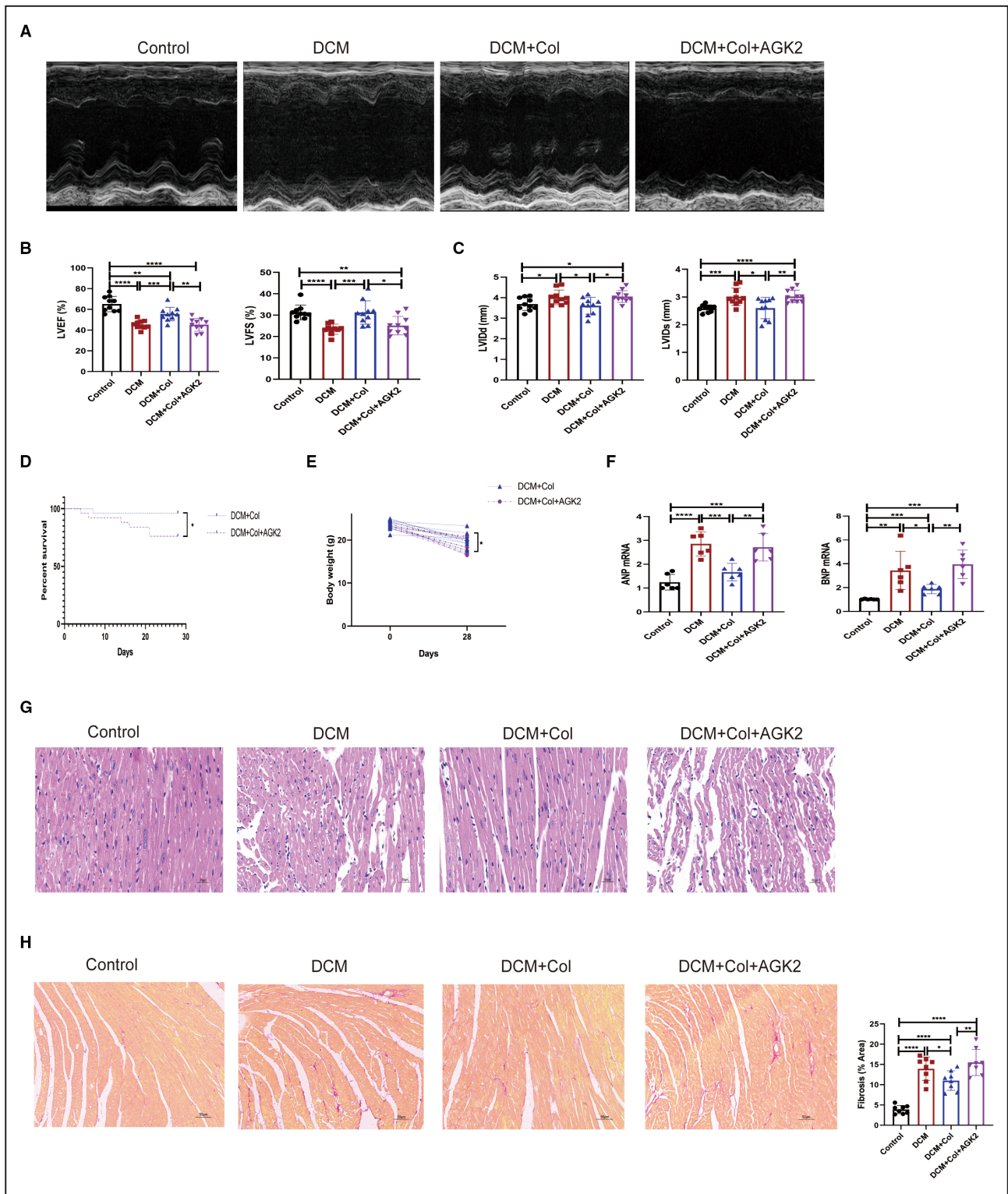
The activation of the NLRP3 inflammasome plays pivotal roles in the pathological process of DCM.[6,35] Accumulating evidence suggests that the NLRP3 inflammasome is the major target of colchicine in acute inflammation stages.[36,37] Low-dose colchicine alters the conformation of tubulin and interferes with the stability of microtubules, preventing the activation of the NLRP3 inflammasome.[37,38] Our findings also showed that colchicine treatment inhibited the doxorubicin-induced increase in cardiac protein expression of the NLRP3 inflammasome pathway, accompanied by a decrease in the proinflammatory cytokine IL-1β during

Figure 6. Inhibition of SIRT2 (Sirtuin 2) abrogates the beneficial effects of colchicine on dilated cardiomyopathy mice.

A through **C**, Cardiac function is analyzed by 2-dimensional murine echocardiography, left ventricular (LV) ejection fraction, LV fractional shortening, LV internal dimensions at end-diastole, and LV internal dimensions at end-systole values are measured at the end point of experiment (n=10 each group). **D**, Kaplan–Meier survival curve for each group mice followed for 4 weeks with or without doxorubicin challenge (n=25 each group). **E**, The changes of body weight from beginning to end (n=10 each group). **F**, Relative expression of *ANP* (atrial natriuretic peptide) mRNA and *BNP* (brain natriuretic peptide) mRNA are normalized to *GAPDH* mRNA in murine cardiac tissues at the end point of experiment. **G** and **H**, The representative hematoxylin and eosin staining (**G**) and Sirius red staining (**H**) of hearts in each group are shown. Quantification of interstitial fibrosis (% area) in hearts is shown on the right; n=8 each group. Five images per mouse are evaluated. Scale bar=50 μm. Data are shown as mean±SEM. Data of (**B**, **C**, and **E** through **G**) are analyzed by 1-way ANOVA (Tukey post-test). Data of (**D**) is analyzed by Mantel-Cox test. ANP indicates atrial natriuretic peptide; BNP, brain natriuretic peptide; DCM, dilated cardiomyopathy; LVEF, left ventricular ejection fraction; LVFS, left ventricular fractional shortening; LVIDd, left ventricular internal dimensions at end-diastole; and LVIDs, left ventricular internal dimensions at end-systole. *$P<0.05$ between groups; **$P<0.01$ between groups; ***$P<0.005$ between groups and ****$P<0.001$ between groups. AGK2 indicates a reversible inhibitor of SIRT2; Col, colchicine.

the chronic inflammatory response. In addition, the number of apoptosis-associated speck-like protein with card domain specks was attenuated by colchicine, suggesting that colchicine interfered with the assembly of the NLRP3 inflammasome in the damaged myocardium.

Sirtuins are involved in a series of physiological events and cellular pathways.[39,40] In particular, SIRT2, as the only cytosolic sirtuin, exhibits a cardioprotective function.[41,42] SIRT2-mediated activation of AMPK prevents aging-related and Ang II-induced cardiac hypertrophy by deacetylating liver kinase B1.[42] In diabetic cardiomyopathy, SIRT2 interferes with the stability of microtubules through α-tubulin deacetylation.[43] An advanced study has shown that SIRT2 participates in the deacetylation of NLRP3 and prevents the assembly of the NLRP3 inflammasome in aging mice.[12] These observations indicate that SIRT2 regulates 2 steps of NLRP3 inflammasome activation, assembly and transport, by deacetylating NLRP3 and tubulin. However, the loss of SIRT2 often occurs under numerous pathological conditions, such as aging, hyperglycemia, and obesity, which might be related to the activation of the NLRP3 inflammasome.[44–46] Our research showed that dysregulation of the NLRP3 inflammasome was associated with the inactivation of SIRT2, leading to chronic inflammation during the DCM process. Colchicine supplementation could significantly protect SIRT2 from inactivation and suppress the aberrant activation of the NLRP3 inflammasome. In addition, downregulation of SIRT2 abolished the colchicine-mediated inhibitory effect on NLRP3 inflammasome activation. Importantly, inhibition of SIRT2 in vivo via AGK2 abrogated the cardioprotective effects of colchicine during the progression of DCM. Since colchicine has been recognized as a depolymerization executor of microtubulin, our research also clarified that colchicine affected the deacetylation of NLRP3 in a SIRT2-dependent manner, indicating that SIRT2 might be the downstream target of colchicine in regulating the activation of the NLRP3 inflammasome.

It is well established that microtubules are major cytoskeletal component of cardiomyocytes, and play an important role in modulating both the electrical and mechanical activities of the heart.[47] Colchicine is served as a microtubule disruptor that has an effect on cardiomyocytes via Ca^{2+} homeostasis in both quiescent and pathological conditions.[48,49] Besides, inhibition of microtubule polymerization by colchicine prevented cardiac gap junction protein connexin-43 remodeling in duchenne muscular dystrophy mice.[16] Caporizzo et al reported that colchicine protected from human heart failure via reducing microtubule density and lowering viscoelasticity in myocytes.[50] Our results of hematoxylin and eosin staining in Figure 1 also demonstrated that colchicine protected the cardiomyocytes from sarcomere disturbance induced by doxorubicin. Together, these studies showed that colchicine has a direct beneficial effect on myocytes in the progression of cardiovascular diseases except the anti-inflammatory actions.

The present research also reported that colchicine was able to prevent the doxorubicin-dependent weight loss and mortality. Apart from improvements of cardiac functions, the other mechanism of colchicine's beneficial effects may be as follows. Firstly, doxorubicin induces the production of excess free radicals and proinflammatory cytokines, which result in the multiple organs toxicities like kidney,[51] liver,[52] and brain.[53] Colchicine has a potent systemic anti-inflammatory ability. Our results showed that the circulating levels of IL1, IL-6, and TNF-α were significantly reduced after colchicine treatment. Some studies reported that colchicine has multi-organs protective effect such as liver[34] and kidney[54] via inhibiting inflammation. Together, colchicine could rescue the weight loss and reduce the mortality partially owing to its anti-inflammatory effects on multi-organs protection. Second, SIRT2, the downstream target of colchicine, has been proven to inhibit the oxidative stress and inflammatory response,[55] which is helpful to reduce the side effects of doxorubicin. Inhibition of SIRT2 by AGK2 administration in vivo abolished the benefits of survival rate and weight loss brought by colchicine during the entire experiments (Figure 6), suggesting that SIRT2

was closely associated with the regulation of colchicine. Third, GDF15 is defined as a central regulator of appetite and a potential target for the treatment of both cancer anorexia and weight loss.[56,57] Kempf et al has identified that loss expression of GDF15 would lead to fatal cardiac rupture after myocardial infarction.[58] Our results showed an increase of circulating GDF15 after colchicine treatment (Figure 2B). These downstream regulators of colchicine contribute to the advantageous effects of colchicine on weight loss and mortality induced by doxorubicin.

In conclusion, these findings reveal that the anti-inflammatory medication colchicine slows the development of DCM through SIRT2-mediated deacetylation of NLRP3, resulting in the suppression of NLRP3 inflammasome activation. Given the low cost and long-term safety of colchicine use, our research provides a theoretical possibility for colchicine application in chronic inflammatory heart failure.

REFERENCES

1. Japp AG, Gulati A, Cook SA, Cowie MR, Prasad SK. The diagnosis and evaluation of dilated cardiomyopathy. *J Am Coll Cardiol*. 2016;67:2996–3010. doi: 10.1016/j.jacc.2016.03.590

2. McNally EM, Mestroni L. Dilated cardiomyopathy: genetic determinants and mechanisms. *Circ Res*. 2017;121:731–748. doi: 10.1161/CIRCRESAHA.116.309396

3. Schultheiss HP, Fairweather D, Caforio ALP, Escher F, Hershberger RE, Lipshultz SE, Liu PP, Matsumori A, Mazzanti A, McMurray J, et al. Dilated cardiomyopathy. *Nat Rev Dis Primers*. 2019;5:32. doi: 10.1038/s41572-019-0084-1

4. Merlo M, Cannata A, Gobbo M, Stolfo D, Elliott PM, Sinagra G. Evolving concepts in dilated cardiomyopathy. *Eur J Heart Fail*. 2018;20:228–239. doi: 10.1002/ejhf.1103

5. Smith ED, Lakdawala NK, Papoutsidakis N, Aubert G, Mazzanti A, McCanta AC, Agarwal PP, Arscott P, Dellefave-Castillo LM, Vorovich EE, et al. Desmoplakin cardiomyopathy, a fibrotic and inflammatory form of cardiomyopathy distinct from typical dilated or arrhythmogenic

6. Zeng C, Duan F, Hu J, Luo B, Huang B, Lou X, Sun X, Li H, Zhang X, Yin S, et al. NLRP3 inflammasome-mediated pyroptosis contributes to the pathogenesis of non-ischemic dilated cardiomyopathy. *Redox Biol*. 2020;34:101523. doi: 10.1016/j.redox.2020.101523

7. Caragnano A, Aleksova A, Bulfoni M, Cervellin C, Rolle IG, Veneziano C, Barchiesi A, Mimmi MC, Vascotto C, Finato N, et al. Autophagy and inflammasome activation in dilated cardiomyopathy. *J Clin Med*. 2019;8:1519. doi: 10.3390/jcm8101519

8. Tardif JC, Kouz S, Waters DD, Bertrand OF, Diaz R, Maggioni AP, Pinto FJ, Ibrahim R, Gamra H, Kiwan GS, et al. Efficacy and safety of low-dose colchicine after myocardial infarction. *N Engl J Med*. 2019;381:2497–2505. doi: 10.1056/NEJMoa1912388

9. Imazio M, Nidorf M. Colchicine and the heart. *Eur Heart J*. 2021;42:2745–2760. doi: 10.1093/eurheartj/ehab221

10. Slobodnick A, Shah B, Pillinger MH, Krasnokutsky S. Colchicine: old and new. *Am J Med*. 2015;128:461–470. doi: 10.1016/j.amjmed.2014.12.010

11. Martinez GJ, Celermajer DS, Patel S. The NLRP3 inflammasome and the emerging role of colchicine to inhibit atherosclerosis-associated inflammation. *Atherosclerosis*. 2018;269:262–271. doi: 10.1016/j.atherosclerosis.2017.12.027

12. He M, Chiang HH, Luo H, Zheng Z, Qiao Q, Wang L, Tan M, Ohkubo R, Mu WC, Zhao S, et al. An acetylation switch of the NLRP3 inflammasome regulates aging-associated chronic inflammation and insulin resistance. *Cell Metab*. 2020;31:580–591.e585. doi: 10.1016/j.cmet.2020.01.009

13. Watroba M, Dudek I, Skoda M, Stangret A, Rzodkiewicz P, Szukiewicz D. Sirtuins, epigenetics and longevity. *Ageing Res Rev*. 2017;40:11–19. doi: 10.1016/j.arr.2017.08.001

14. Youm YH, Nguyen KY, Grant RW, Goldberg EL, Bodogai M, Kim D, D'Agostino D, Planavsky N, Lupfer C, Kanneganti TD, et al. The ketone metabolite beta-hydroxybutyrate blocks NLRP3 inflammasome-mediated inflammatory disease. *Nat Med*. 2015;21:263–269. doi: 10.1038/nm.3804

15. Podyacheva EY, Kushnareva EA, Karpov AA, Toropova YG. Analysis of models of doxorubicin-induced cardiomyopathy in rats and mice. A modern view from the perspective of the pathophysiologist and the clinician. *Front Pharmacol*. 2021;12:670479. doi: 10.3389/fphar.2021.670479

16. Himelman E, Lillo MA, Nouet J, Gonzalez JP, Zhao Q, Xie LH, Li H, Liu T, Wehrens XH, Lampe PD, et al. Prevention of connexin-43 remodeling protects against duchenne muscular dystrophy cardiomyopathy. *J Clin Invest*. 2020;130:1713–1727. doi: 10.1172/JCI128190

17. Li DJ, Sun SJ, Fu JT, Ouyang SX, Zhao QJ, Su L, Ji QX, Sun DY, Zhu JH, Zhang GY, et al. NAD(+)-boosting therapy alleviates nonalcoholic fatty liver disease via stimulating a novel exerkine Fndc5/irisin. *Theranostics*. 2021;11:4381–4402. doi: 10.7150/thno.53652

18. Herster F, Bittner Z, Archer NK, Dickhofer S, Eisel D, Eigenbrod T, Knorpp T, Schneiderhan-Marra N, Loffler MW, Kalbacher H, et al. Neutrophil extracellular trap-associated RNA and LL37 enable self-amplifying inflammation in psoriasis. *Nat Commun*. 2020;11:105. doi: 10.1038/s41467-019-13756-4

19. He WT, Wan H, Hu L, Chen P, Wang X, Huang Z, Yang ZH, Zhong CQ, Han J. Gasdermin D is an executor of pyroptosis and required for interleukin-1beta secretion. *Cell Res*. 2015;25:1285–1298. doi: 10.1038/cr.2015.139

20. Zhang C, Chen B, Guo A, Zhu Y, Miller JD, Gao S, Yuan C, Kutschke W, Zimmerman K, Weiss RM, et al. Microtubule-mediated defects in junctophilin-2 trafficking contribute to myocyte transverse-tubule remodeling and Ca^{2+} handling dysfunction in heart failure. *Circulation*. 2014;129:1742–1750. doi: 10.1161/CIRCULATIONAHA.113.008452

21. Misawa T, Takahama M, Kozaki T, Lee H, Zou J, Saitoh T, Akira S. Microtubule-driven spatial arrangement of mitochondria promotes activation of the NLRP3 inflammasome. *Nat Immunol*. 2013;14:454–460. doi: 10.1038/ni.2550

22. Li M, Duan L, Cai YL, Li HY, Hao BC, Chen JQ, Liu HB. Growth differentiation factor-15 is associated with cardiovascular outcomes in patients with coronary artery disease. *Cardiovasc Diabetol*. 2020;19:120. doi: 10.1186/s12933-020-01092-7

23. Lok SI, Winkens B, Goldschmeding R, van Geffen AJ, Nous FM, van Kuik J, van der Weide P, Klopping C, Kirkels JH, Lahpor JR, et al. Circulating growth differentiation factor-15 correlates with myocardial fibrosis in patients with non-ischaemic dilated cardiomyopathy and

right ventricular cardiomyopathy. *Circulation*. 2020;141:1872–1884. doi: 10.1161/CIRCULATIONAHA.119.044934

decreases rapidly after left ventricular assist device support. *Eur J Heart Fail*. 2012;14:1249–1256. doi: 10.1093/eurjhf/hfs120

24. Sun X, Shan A, Wei Z, Xu B. Intravenous mesenchymal stem cell-derived exosomes ameliorate myocardial inflammation in the dilated cardiomyopathy. *Biochem Biophys Res Commun*. 2018;503:2611–2618. doi: 10.1016/j.bbrc.2018.08.012

25. Zhang H, Xu A, Sun X, Yang Y, Zhang L, Bai H, Ben J, Zhu X, Li X, Yang Q, et al. Self-maintenance of cardiac resident reparative macrophages attenuates doxorubicin-induced cardiomyopathy through the SR-A1-c-myc axis. *Circ Res*. 2020;127:610–627. doi: 10.1161/CIRCRESAHA.119.316428

26. Fernandez-Ruiz I. Low-dose colchicine shows promise in chronic coronary disease. *Nat Rev Cardiol*. 2020;17:680–681. doi: 10.1038/s41569-020-00456-6

27. Deftereos S, Giannopoulos G, Panagopoulou V, Bouras G, Raisakis K, Kossyvakis C, Karageorgiou S, Papadimitriou C, Vastaki M, Kaoukis A, et al. Anti-inflammatory treatment with colchicine in stable chronic heart failure: a prospective, randomized study. *JACC Heart Fail*. 2014;2:131–137. doi: 10.1016/j.jchf.2013.11.006

28. Wu Q, Liu H, Liao J, Zhao N, Tse G, Han B, Chen L, Huang Z, Du Y. Colchicine prevents atrial fibrillation promotion by inhibiting IL-1beta-induced IL-6 release and atrial fibrosis in the rat sterile pericarditis model. *Biomed Pharmacother*. 2020;129:110384. doi: 10.1016/j.biopha.2020.110384

29. Shah B, Pillinger M, Zhong H, Cronstein B, Xia Y, Lorin JD, Smilowitz NR, Feit F, Ratnapala N, Keller NM, et al. Effects of acute colchicine administration prior to percutaneous coronary intervention: COLCHICINE-PCI randomized trial. *Circ Cardiovasc Interv*. 2020;13:e008717. doi: 10.1161/CIRCINTERVENTIONS.119.008717

30. Martini E, Kunderfranco P, Peano C, Carullo P, Cremonesi M, Schorn T, Carriero R, Termanini A, Colombo FS, Jachetti E, et al. Single-cell sequencing of mouse heart immune infiltrate in pressure overload-driven heart failure reveals extent of immune activation. *Circulation*. 2019;140:2089–2107. doi: 10.1161/CIRCULATIONAHA.119.041694

31. Vaidya K, Tucker B, Kurup R, Khandkar C, Pandzic E, Barraclough J, Machet J, Misra A, Kavurma M, Martinez G, et al. Colchicine inhibits neutrophil extracellular trap formation in patients with acute coronary syndrome after percutaneous coronary intervention. *J Am Heart Assoc*. 2021;10:e018993. doi: 10.1161/JAHA.120.018993

32. Xu J, Kimball TR, Lorenz JN, Brown DA, Bauskin AR, Klevitsky R, Hewett TE, Breit SN, Molkentin JD. GDF15/MIC-1 functions as a protective and antihypertrophic factor released from the myocardium in association with SMAD protein activation. *Circ Res*. 2006;98:342–350. doi: 10.1161/01.RES.0000202804.84885.d0

33. May BM, Kochi AN, Magalhaes APA, Scolari F, Zimerman A, Andrades M, Zimerman LI, Rohde LE, Pimentel M. Growth/differentiation factor-15 (GDF-15) as a predictor of serious arrhythmic events in patients with nonischemic dilated cardiomyopathy. *J Electrocardiol*. 2022;70:19–23. doi: 10.1016/j.jelectrocard.2021.10.002

34. Weng JH, Koch PD, Luan HH, Tu HC, Shimada K, Ngan I, Ventura R, Jiang R, Mitchison TJ. Colchicine acts selectively in the liver to induce hepatokines that inhibit myeloid cell activation. *Nat Metab*. 2021;3:513–522. doi: 10.1038/s42255-021-00366-y

35. Wei S, Ma W, Zhang B, Li W. NLRP3 inflammasome: a promising therapeutic target for drug-induced toxicity. *Front Cell Dev Biol*. 2021;9:634607. doi: 10.3389/fcell.2021.634607

36. Leung YY, Yao Hui LL, Kraus VB. Colchicine—update on mechanisms of action and therapeutic uses. *Semin Arthritis Rheum*. 2015;45:341–350. doi: 10.1016/j.semarthrit.2015.06.013

37. Wang Y, Viollet B, Terkeltaub R, Liu-Bryan R. AMP-activated protein kinase suppresses urate crystal-induced inflammation and transduces colchicine effects in macrophages. *Ann Rheum Dis*. 2016;75:286–294. doi: 10.1136/annrheumdis-2014-206074

38. Dubey KK, Kumar P, Labrou NE, Shukla P. Biotherapeutic potential and mechanisms of action of colchicine. *Crit Rev Biotechnol*. 2017;37:1038–1047. doi: 10.1080/07388551.2017.1303804

39. Matsushima S, Sadoshima J. The role of sirtuins in cardiac disease. *Am J Physiol Heart Circ Physiol*. 2015;309:H1375–H1389. doi: 10.1152/ajpheart.00053.2015

40. Singh CK, Chhabra G, Ndiaye MA, Garcia-Peterson LM, Mack NJ, Ahmad N. The role of sirtuins in antioxidant and redox signaling. *Antioxid Redox Signal*. 2018;28:643–661. doi: 10.1089/ars.2017.7290

41. Zhao L, Qi Y, Xu L, Tao X, Han X, Yin L, Peng J. MicroRNA-140-5p aggravates doxorubicin-induced cardiotoxicity by promoting myocardial oxidative stress via targeting Nrf2 and Sirt2. *Redox Biol*. 2018;15:284–296. doi: 10.1016/j.redox.2017.12.013

42. Tang X, Chen XF, Wang NY, Wang XM, Liang ST, Zheng W, Lu YB, Zhao X, Hao DL, Zhang ZQ, et al. SIRT2 acts as a cardioprotective deacetylase in pathological cardiac hypertrophy. *Circulation*. 2017;136:2051–2067. doi: 10.1161/CIRCULATIONAHA.117.028728

43. Yuan Q, Zhan L, Zhou QY, Zhang LL, Chen XM, Hu XM, Yuan XC. SIRT2 regulates microtubule stabilization in diabetic cardiomyopathy. *Eur J Pharmacol*. 2015;764:554–561. doi: 10.1016/j.ejphar.2015.07.045

44. Kida Y, Goligorsky MS. Sirtuins, cell senescence, and vascular aging. *Can J Cardiol*. 2016;32:634–641. doi: 10.1016/j.cjca.2015.11.022

45. Watanabe H, Inaba Y, Kimura K, Matsumoto M, Kaneko S, Kasuga M, Inoue H. Sirt2 facilitates hepatic glucose uptake by deacetylating glucokinase regulatory protein. *Nat Commun*. 2018;9:30. doi: 10.1038/s41467-017-02537-6

46. Krishnan J, Danzer C, Simka T, Ukropec J, Walter KM, Kumpf S, Mirtschink P, Ukropcova B, Gasperikova D, Pedrazzini T, et al. Dietary obesity-associated Hif1α activation in adipocytes restricts fatty acid oxidation and energy expenditure via suppression of the Sirt2-NAD+ system. *Genes Dev*. 2012;26:259–270. doi: 10.1101/gad.180406.111

47. Caporizzo MA, Chen CY, Prosser BL. Cardiac microtubules in health and heart disease. *Exp Biol Med*. 2019;244:1255–1272. doi: 10.1177/1535370219868960

48. Kerfant BG, Vassort G, Gomez AM. Microtubule disruption by colchicine reversibly enhances calcium signaling in intact rat cardiac myocytes. *Circ Res*. 2001;88:E59–E65. doi: 10.1161/hh0701.090462

49. Lu YY, Chen YC, Kao YH, Lin YK, Yeh YH, Chen SA, Chen YJ. Colchicine modulates calcium homeostasis and electrical property of HL-1 cells. *J Cell Mol Med*. 2016;20:1182–1190. doi: 10.1111/jcmm.12818

50. Caporizzo MA, Chen CY, Bedi K, Margulies KB, Prosser BL. Microtubules increase diastolic stiffness in failing human cardiomyocytes and myocardium. *Circulation*. 2020;141:902–915. doi: 10.1161/CIRCULATIONAHA.119.043930

51. El-Sayed EM, Mansour AM, El-Sawy WS. Protective effect of proanthocyanidins against doxorubicin-induced nephrotoxicity in rats. *J Biochem Mol Toxicol*. 2017;31:e21965. doi: 10.1002/jbt.21965

52. Jacevic V, Djordjevic A, Srdjenovic B, Milic-Tores V, Segrt Z, Dragojevic-Simic V, Kuca K. Fullerenol nanoparticles prevents doxorubicin-induced acute hepatotoxicity in rats. *Exp Mol Pathol*. 2017;102:360–369. doi: 10.1016/j.yexmp.2017.03.005

53. Tangpong J, Cole MP, Sultana R, Estus S, Vore M, St Clair W, Ratanachaiyavong S, St Clair DK, Butterfield DA. Adriamycin-mediated nitration of manganese superoxide dismutase in the central nervous system: insight into the mechanism of chemobrain. *J Neurochem*. 2007;100:191–201. doi: 10.1111/j.1471-4159.2006.04179.x

54. Kim S, Jung ES, Lee J, Heo NJ, Na KY, Han JS. Effects of colchicine on renal fibrosis and apoptosis in obstructed kidneys. *Korean J Intern Med*. 2018;33:568–576. doi: 10.3904/kjim.2016.131

55. Qu ZA, Ma XJ, Huang SB, Hao XR, Li DM, Feng KY, Wang WM. SIRT2 inhibits oxidative stress and inflammatory response in diabetic osteoarthritis. *Eur Rev Med Pharmacol Sci*. 2020;24:2855–2864. doi: 10.26355/eurrev_202003_20649

56. Ahmed DS, Isnard S, Lin J, Routy B, Routy JP. GDF15/GFRAL pathway as a metabolic signature for cachexia in patients with cancer. *J Cancer*. 2021;12:1125–1132. doi: 10.7150/jca.50376

57. Johnen H, Lin S, Kuffner T, Brown DA, Tsai VW, Bauskin AR, Wu L, Pankhurst G, Jiang L, Junankar S, et al. Tumor-induced anorexia and weight loss are mediated by the TGF-beta superfamily cytokine MIC-1. *Nat Med*. 2007;13:1333–1340. doi: 10.1038/nm1677

58. Kempf T, Zarbock A, Widera C, Butz S, Stadtmann A, Rossaint J, Bolomini-Vittori M, Korf-Klingebiel M, Napp LC, Hansen B, et al. GDF-15 is an inhibitor of leukocyte integrin activation required for survival after myocardial infarction in mice. *Nat Med*. 2011;17:581–588. doi: 10.1038/nm.2354

SUPPLEMENTAL MATERIAL

Figure S1. Mice of colchicine treatment alone did not show any difference compared with the control mice in cardiac function.
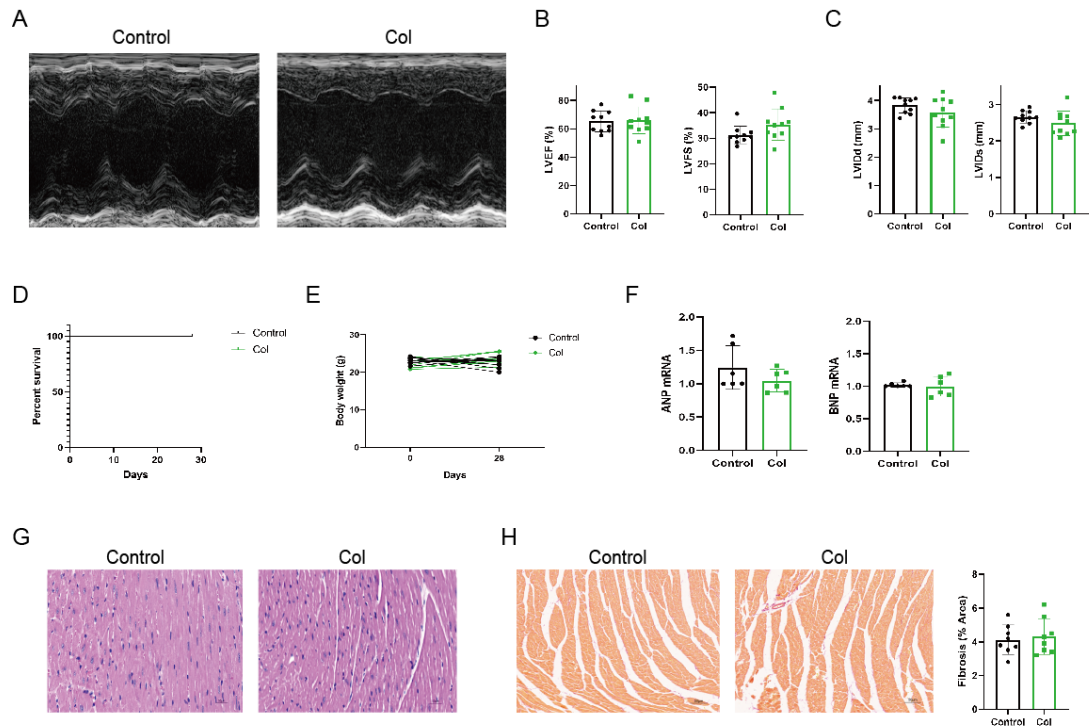

A-C. Cardiac function was analyzed by two-dimensional murine echocardiography, LVEF, LVFS, LVIDd and LVIDs values were measured at the endpoint of experiment (n=10 each group). **D.** Kaplan-Meier survival curve for each group mice followed for 4 weeks (n=10 each group). **E.** The changes of body weight from beginning to end (n=10 each group). **F.** Relative expression of *ANP* mRNA and *BNP* mRNA were normalized to *GAPDH* mRNA in murine cardiac tissues at the endpoint of experiment. **G-H.** The representative HE staining (H) and Sirius red staining (I) of hearts in each group were shown. Quantification of interstitial fibrosis (% area) in hearts was shown on the right. N=8 each group. 5 images per mouse were evaluated. Scale bar=50μm. Data were shown as mean± SEM. Data of **B-C, E-F** and **H** were analyzed by Stendent's t test. Data of **D** was analyzed by Mantel-Cox test. *p < 0.05 between groups;**p < 0.01 between groups; ***p < 0.005 between groups and ****p < 0.001 between groups.

Figure S2. Flow cytometry gating strategy in tissues and isolated neutrophils.
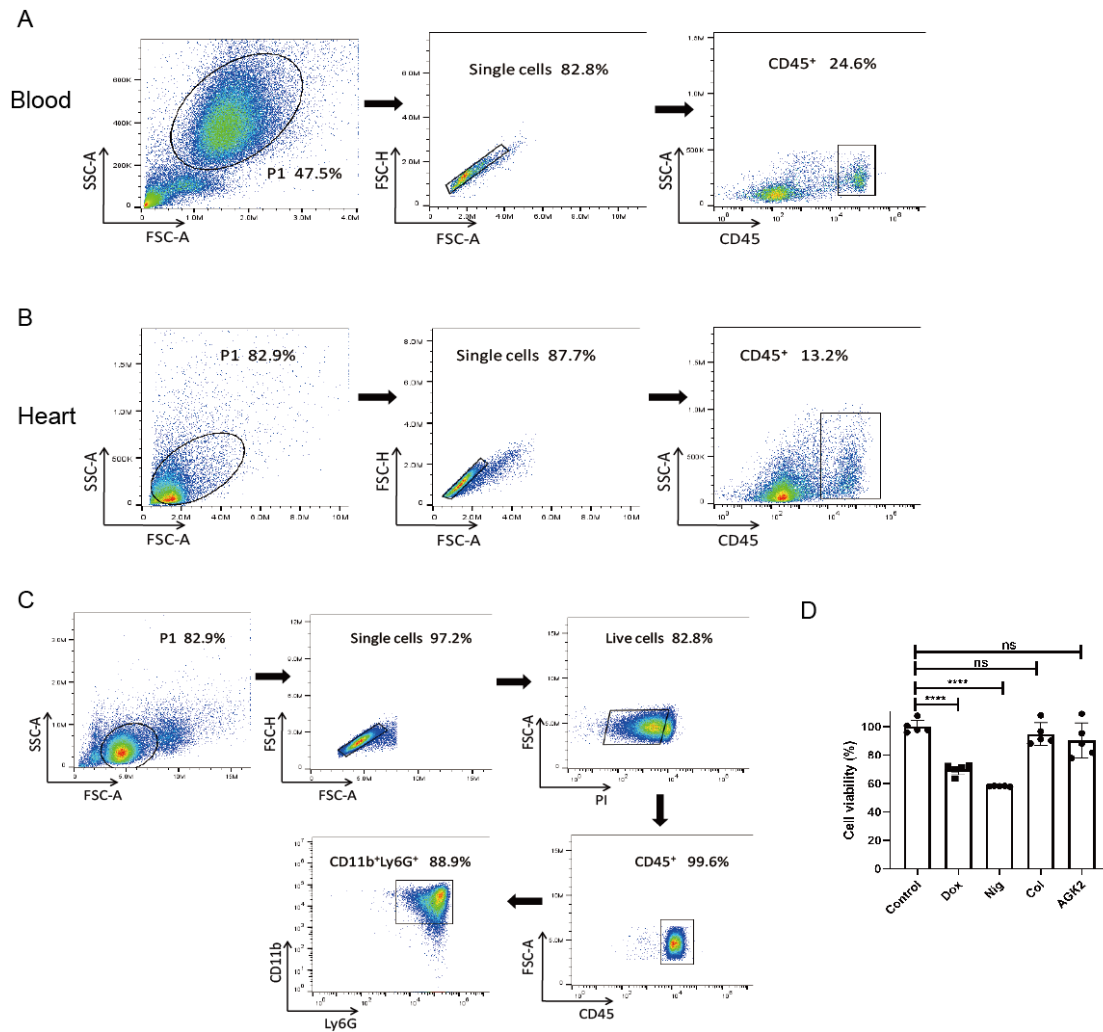
A-B. Flow cytometry gating strategy utilized to identify and characterize CD45$^+$ cells populations in the blood and hearts of mice. **C.** Primary neutrophils isolated from bone marrow via magnetic bead separator were identified for purity by flow cytometry. **D.** Impacts of drug treatments on the viability of isolated neutrophils that were treated +/- colchicine (10μM, 4h), +/- SIRT2 inhibitor AGK2 (10μM, 4h) or challenged with doxorubicin (5μM, 4h) and inflammasome activators nigericin (10μM, 4h). Data were representative of five independent experiments. Data were shown as mean± SEM. Statistical significance was determined by Stendent's t test compared between the drug treatment groups and the control group. *p < 0.05 between groups;**p < 0.01 between groups; ***p < 0.005 between groups ; and ****p < 0.001 between groups.

Figure S3. The expression of tissue SIRT2 was reduced by inhibitor AGK2 stimuli.

A
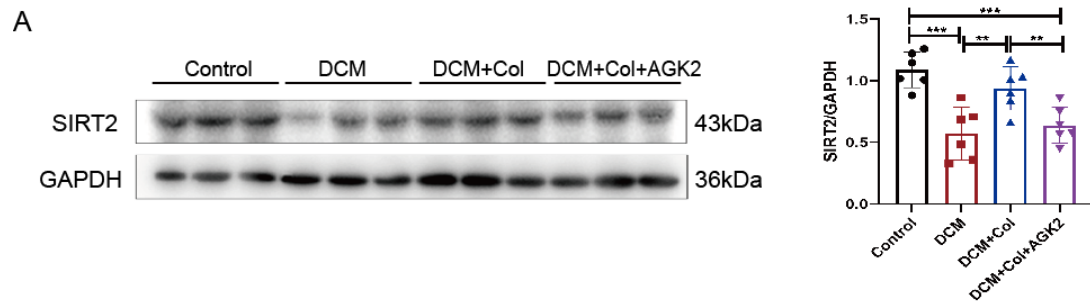
A. SIRT2 protein expression of cardiac tissues was detected by immunoblots and the analysis was shown on the right. Data are shown as mean± SEM. Data are analyzed by one-way ANOVA (Tukey's post-test)